



## All Solid-State Li/Li<sub>x</sub>MnO<sub>2</sub> Polymer Battery Using Ceramic Modified Polymer Electrolytes

Congxiao Wang,<sup>z</sup> Yongyao Xia, Kenichi Koumoto, and Tetsuo Sakai\*

National Institute of Advanced Industrial Science and Technology Kansai Collaboration Center,  
Research Team of Secondary Battery System, Ikeda, Osaka 563-8577, Japan

The addition of ceramics to the polymer electrolyte was found to result in an enhancement of the ionic conductivity, especially at temperatures below the crystalline-amorphous transition (normally at 60°C), as well as the mechanical property, consistent with other previously reported studies. The electrochemical profile of an all solid-state Li/Li<sub>x</sub>MnO<sub>2</sub> based on the ceramics-modified and ceramics-free poly(ethylene oxide) (PEO)-LiClO<sub>4</sub> electrolyte has also been studied. We found that the addition of some ceramics, e.g., the metal oxides, could suppress the decomposition of PEO toward the cathode thus showing an improved charge/discharge efficiency upon cycling of an all solid-state Li/Li<sub>x</sub>MnO<sub>2</sub>. This improved behavior is most likely linked to the fact that the metal oxide additive can form a stable interaction between the ceramic and the PEO segment, thus stabilizing the PEO structure, and protecting the PEO from oxidation.

© 2002 The Electrochemical Society. [DOI: 10.1149/1.1486239] All rights reserved.

Manuscript submitted July 30, 2001. revised manuscript received February 23, 2002. Available electronically June 12, 2002.

All solid-state lithium/polymer battery (LPB) using a metallic lithium anode and solvent-free polymer electrolyte has been demonstrated to be the most promising secondary battery for electric vehicle applications because of its low risk of liquid electrolyte leakage, higher energy density, and shape flexibility compared to other systems. The main problems that are still to be solved are related to a low conductivity at ambient temperature. Many efforts have been devoted to the development and improvement of the electrolyte's ionic conductivity for such batteries.<sup>1-6</sup> One of the most successful approaches is to add a small-particle size ceramic powder in the polymer electrolyte.<sup>7-10</sup> Most studies have focused primarily on investigating the influence of the addition of ceramic powders on the ionic conductivity and interfacial stability with lithium. Indeed, these new types of composite polymer electrolytes result in an increase in the ionic conductivity and enhanced lithium/polymer-electrolyte interface stability. However, very few studies have been devoted to measure its electrochemical profile in a real battery system, specially the electrochemical stability of the polymer electrolyte on a cathode. The high ionic conductivity and interface stability with lithium is of primary importance when it was applied into a lithium/polymer battery in combination with a composite cathode, and the electrochemical stability against a high voltage is also important. Until now, the evaluation of the electrochemical stability was normally characterized by linear sweep voltammetry (LSV) or cyclic voltammetry (CV) of the polymer electrolyte on a smooth stainless steel blocking electrode. The polymer electrolytes with or without the ceramic additive have been reported to be stable at least above 4 V vs. Li/Li<sup>+</sup>.<sup>4,6</sup> However, when a composite electrolyte works as an electrolyte separator combined with a positive electrode in a real battery system, it contacts the porous composite electrode containing active material and conductive material, e.g., carbon black, acetylene black, graphite, etc., rather than a smooth inert electrode. In the present study, we are interested in investigating the battery performance of the Li/Li<sub>x</sub>MnO<sub>2</sub> cell based on the ceramic-additive polymer electrolyte, rather than the ion conductivity evaluation. We found that some of the ceramic modified composite polymer electrolytes behave in a manner similar to that of the ceramic-free polymer electrolyte, showing a poor charge/discharge efficiency due to poly(ethylene oxide) (PEO) decomposition during cycling even they showed increased ionic conductivity, whereas the PEO decomposition suppression was observed on these doped components which form a stable interreaction between the ceramic surface and the PEO segment. The possible PEO decomposition mechanism was discussed.

### Experimental

PEO (Aldrich Chemical Co.,  $4 \times 10^6$  average molecular weight) and battery-grade LiClO<sub>4</sub> (Tomiya Pure Chemical Industries, Ltd.) were dried under vacuum for 24 h before use. All the ceramic powders were dried at 150°C under vacuum for 24 h. Table I summarizes some properties of these ceramic powders. A high molecular weight branched poly[ethylene oxide-co-(2-methoxyethoxy)ethyl glycidyl ether-co-allylglycidyl ether] [PEO(EO/EM-2/AGE), Mw  $\approx 10^6$ ] with a lithium bis(trifluoromethyl sulfonyl)imide [LiN(CF<sub>3</sub>SO<sub>2</sub>)<sub>2</sub>] electrolyte film was provided by Daiso Co., Ltd., Japan. Its structure is shown in Fig. 1. The cathode material, Li<sub>0.33</sub>MnO<sub>2</sub>, was prepared by preheating a mixture of LiNO<sub>3</sub> and MnO<sub>2</sub> at 260°C for 5 h, followed by heating at 320°C for 12 h in air.<sup>11,12</sup>

All the polymer electrolytes used here were prepared by either the well-known solvent-casting or hot-pressing techniques. The preparation by hot pressing comprised the following procedure: Proper amounts of PEO and ceramic powders were first thoroughly mixed by ballmilling, then a proper amount of lithium salt at an EO/Li ratio of 20/1 was added and mixed by ballmilling again in a dry room. The mixture was then placed between two Mylar sheets, followed by pressing at  $9.8 \times 10^5$  Pa for 10 min at 80°C, then slowly cooled to room temperature. The typical thickness of the polymer electrolyte film was 50 or 100  $\mu$ m. If prepared by the solvent-casting process, it involved dispersing the ceramic powders and the lithium salt in acetonitrile. The solution was stirred for 24 h at room temperature. A known amount of PEO was then added and the solution was continuously stirred for another 24 h to get a homogeneous mixture. The mixture was cast on a Mylar sheet. The solvent was allowed to evaporate at room temperature for 24 h, then was vacuum dried at room temperature to give an electrolyte film with an average 100  $\mu$ m thickness. The electrolyte film was then vacuum dried at 80°C for 24 h.

The conductivity of the polymer-electrolyte film was measured by ac impedance by placing the sample in a two-blocking electrode (stainless steel) cell. The electrode area was 1 cm<sup>2</sup>. The ac impedance experiments were carried out from 25 to 100°C using an EG&G PAR potentiostat coupled with a model 1250 frequency response analyzer controlled by a computer. The impedance spectra were normally recorded from 100 kHz to 0.1 Hz, and the ac oscillation amplitude was 5 mV. The mechanical properties of the selected ceramic-additive composite electrolyte and ceramic-free electrolyte were also evaluated by monitoring the resistance change over time at 60°C.

The preparation process of the composite cathode is described as follows: 65 wt % active material, 5 wt % carbon (Ketjen black), and

\* Electrochemical Society Active Member.

<sup>z</sup> E-mail: Congxiao-wan@aist.go.jp



Table II. Properties of composite electrolyte films.

Additives	Amount (wt %)	Conductivity (s/cm)			Mechanical property	<sup>d</sup> Cycle number of stating decomposition
		40°C	60°C	90°C		
PEO(Aldrich)		$2.17 \times 10^{-6}$	$1.99 \times 10^{-4}$	$1.07 \times 10^{-3}$	× <sup>c</sup>	12
Al <sub>2</sub> O <sub>3</sub>	10	$5.83 \times 10^{-6}$	$2.89 \times 10^{-4}$	$1.13 \times 10^{-3}$	⊙ <sup>a</sup>	100
SiO <sub>2</sub>	10	$8.50 \times 10^{-6}$	$2.42 \times 10^{-4}$	$1.20 \times 10^{-3}$	⊙	>200
TiO <sub>2</sub>	10	$5.29 \times 10^{-6}$	$2.32 \times 10^{-4}$	$1.15 \times 10^{-3}$	⊙	>180
Y <sub>2</sub> O <sub>3</sub>	10	$2.50 \times 10^{-6}$	$2.38 \times 10^{-4}$	$1.03 \times 10^{-3}$	⊙	90
ZrO <sub>2</sub>	10	$6.45 \times 10^{-6}$	$2.36 \times 10^{-4}$	$1.33 \times 10^{-3}$	⊙	>225
γ-LiAlO <sub>2</sub>	10	$3.08 \times 10^{-5}$	$5.44 \times 10^{-4}$	$3.25 \times 10^{-3}$	○ <sup>b</sup>	27
Li <sub>2</sub> SiO <sub>3</sub>	10	$7.25 \times 10^{-6}$	$2.85 \times 10^{-4}$	$9.75 \times 10^{-4}$	⊙	8
Li <sub>2</sub> TiO <sub>3</sub>	10	$3.55 \times 10^{-6}$	$3.40 \times 10^{-4}$	$1.36 \times 10^{-3}$	⊙	7
Li <sub>2</sub> ZrO <sub>3</sub>	10	$1.47 \times 10^{-6}$	$2.06 \times 10^{-4}$	$7.24 \times 10^{-4}$	⊙	6
LiBO <sub>2</sub>	10	$1.03 \times 10^{-5}$	$2.58 \times 10^{-4}$	$9.70 \times 10^{-4}$	⊙	4
Li <sub>2</sub> B <sub>4</sub> O <sub>7</sub>	10	$1.03 \times 10^{-5}$	$2.51 \times 10^{-4}$	$1.04 \times 10^{-3}$	⊙	5
(LiLa)TiO <sub>3</sub>	10	$3.82 \times 10^{-6}$	$2.77 \times 10^{-4}$	$8.91 \times 10^{-4}$	○	1
Li <sub>3</sub> PO <sub>4</sub>	10	$8.20 \times 10^{-6}$	$2.53 \times 10^{-4}$	$9.01 \times 10^{-4}$	○	4
BaTiO <sub>3</sub>	1.5	$3.20 \times 10^{-5}$	$2.94 \times 10^{-4}$	$1.13 \times 10^{-3}$	○	50
CaTiO <sub>3</sub>	1.5	$3.63 \times 10^{-5}$	$3.18 \times 10^{-4}$	$1.21 \times 10^{-3}$	○	90
PbTiO <sub>3</sub>	1.5	$6.85 \times 10^{-6}$	$2.81 \times 10^{-4}$	$1.10 \times 10^{-3}$	⊙	>120
SrTiO <sub>3</sub>	1.5	$1.81 \times 10^{-5}$	$2.83 \times 10^{-4}$	$8.70 \times 10^{-4}$	⊙	87

<sup>a</sup> ⊙ Good.<sup>b</sup> ○ Fair.<sup>c</sup> × Poor.<sup>d</sup> Coulombic efficiency  $\eta < 98\%$ .

**Mechanical property.**—It has been generally suggested that improving the ionic conductivity of the PEO-based electrolytes can be done by one of the following approaches: (i) preparation of cross-linked polymer networks, random, block or comb-like copolymers with short chains of ethylene oxide (type 1); (ii) utilization of organic plasticizers (type 2); and (iii) preparation of an inorganic/organic composite electrolyte by ceramic additives (type 3). Among these systems with improved conductivity, some show an increase without a reduction in their mechanical properties, such as types 1 and 3. The others, such as type 2, suffer from poor mechanical strength. Good mechanical strength is required for use as an electrolyte separator in the lithium/polymer battery production process. The mechanical properties of the SiO<sub>2</sub>-additive composite polymer electrolyte was investigated in comparison with the ceramic-free electrolyte according to the method suggested by Weston *et al.*<sup>15</sup> Basically, it consists of monitoring the resistance responses of a polymer electrolyte film between two blocking electrodes as a function of the storage time at constant temperature and pressure (at  $1.0 \times 10^5$  Pa). Any mechanical degradation of the polymer electrolyte would result in a thickness reduction and thus give rise to a decrease in the overall cell resistance. To exclude any thermal history effect,<sup>16</sup> all the polymer electrolytes prepared either by the hot-pressing or solvent-casting techniques were annealed at 100°C for 24 h. Table III shows the cell resistance of a 100  $\mu$ m thick SiO<sub>2</sub>-additive and ceramic-free polymer membranes at the initial state and after 93 h. The results in Table III definitely reveal that the ceramic additive composite has a much better thermal resistivity behavior, indicative of the better mechanical properties. All data were obtained from ac impedance measurements.

As demonstrated above, a significant improvement in the lithium metal anode cycle efficiency was found when lithium was in contact with a solid-state polymer electrolyte because polymer electrolytes have relatively slower reaction kinetics with lithium metal. However, note that improvement does not mean that dendritic growth is totally absent. We believe that the mechanical property is one of the major factors affecting the dendritic growth. Figure 4 compares the charge curve of symmetric Li/SPE/Li cells containing a 10% SiO<sub>2</sub> additive and ceramic-free polymer films (50  $\mu$ m in thickness) at 60°C. It shows very flat curves over 10 h at a current density of

0.1 mA/cm<sup>2</sup>. However, a sudden voltage drop from 0.2 to 0 V vs. Li/Li<sup>+</sup> was observed after 0.5 h for the ceramic-free PEO electrolyte (a), and at 5.8 h for the SiO<sub>2</sub>-additive composite electrolyte (b) when a current of 0.4 mA/cm<sup>2</sup> was applied. This is due to the formation of lithium dendrites during the charge (lithium plating), which further destroys the separator and causes the cell to short. In summary, the better mechanical property of the ceramic-additive composite electrolyte may provide a thin electrolyte film for high power lithium/polymer batteries.

**Electrochemical stability with a composite cathode.**—Figure 5 shows the charge/discharge curves of a Li/SPE/Li<sub>0.33</sub>MnO<sub>2</sub> cell at 60°C containing the ceramic-free electrolyte for the first 15 cycles. The active material mass loading is 5 mg/cm<sup>2</sup>, and the current density examined here was 0.25 mA/cm<sup>2</sup> corresponding to C/3. Li<sub>0.33</sub>MnO<sub>2</sub> delivers a rechargeable capacity of 150 mAh/g with a very flat potential plateau at ca. 2.9 V vs. Li/Li<sup>+</sup> at the C/3 rate corresponding to a specific energy of 435 Wh/kg of the pure oxide. A large charge capacity over discharge capacity was observed at cycle 14, which is most likely due to the decomposition of PEO. A plot of the charge/discharge capacity vs. cycle number is given in Fig. 6A. A poor charge/discharge efficiency was observed starting at cycle 12 with the poorest at cycle 20, but improved later, and disappeared at cycle 40. Figure 6B and C also show the cycling life test of a Li/solid polymer electrolyte/Li<sub>0.33</sub>MnO<sub>2</sub> cell at 60°C containing  $\gamma$ -LiAlO<sub>2</sub> and SiO<sub>2</sub>-additive polymer electrolytes. The  $\gamma$ -LiAlO<sub>2</sub>-additive electrolyte behaves in a manner similar to the ceramic-free PEO polymer electrolyte and shows a poor charge/discharge efficiency after the 27th cycle, whereas SiO<sub>2</sub> shows a significant enhancement in the cycling profile. It should be noted that it is impossible to detect the above phenomenon by the tradition LSV or CV method, which is normally carried out during the first several cycles. Table II summarizes the cycle during which the polymer-electrolyte decomposition appeared (if discharge/charge efficiency is  $\eta < 98\%$ ) for Li/solid polymer electrolyte/Li<sub>0.33</sub>MnO<sub>2</sub> cells containing various ceramic-additive composite electrolytes. It is evident that metal oxide modification can suppress the PEO decomposition, whereas inorganic lithium salts may somewhat accel-

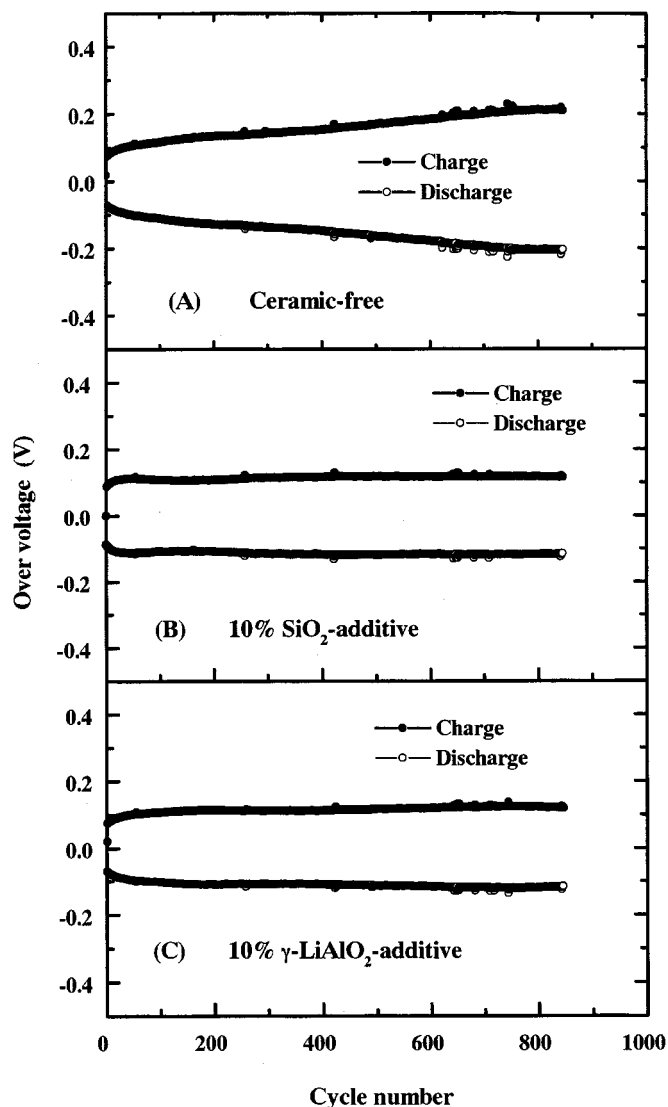


**Figure 3.** Change in the overvoltage upon cycling of symmetric Li/solid polymer electrolyte/Li cells containing various electrolyte membranes at 60°C. (A)  $(\text{PEO})_8\text{LiClO}_4$ , (B)  $(\text{PEO})_8\text{LiClO}_4 + 10\% \text{SiO}_2$ , and (C)  $(\text{PEO})_8\text{LiClO}_4 + 10\% \gamma\text{-LiAlO}_2$ . Charge/discharge current density:  $0.1 \text{ mA/cm}^2$ ,  $Q_D = Q_C = 0.1 \text{ C}$ .

erate the PEO decomposition. The enhancements are in the following order: metal oxides > ferroelectric ceramics > inorganic lithium salts.

It is believed that ceramic addition will not reduce its electrochemical stability, and it is quite interesting to clarify why such differences were detected. It is now well established that the type and growth of the lithium passivation layer is unpredictably influenced by the presence of liquid components and/or impurities in the electrolyte, thereby severely affecting the cyclability of the lithium

**Table III. Mechanical stability of solid polymer electrolyte.**

Sample	Time $t$ at		Initial cell $R_i$ ( $\Omega$ )	Final cell $R_g$ ( $\Omega$ )	Amount of creep $[(R_i - R_g/R_i)] \times 100$ (%)
	$T$ ( $^\circ\text{C}$ )	$T$ (h)			
PEO	60	93	50.2	18.5	63
PEO + $\text{SiO}_2$ (10 wt %)	60	93	77.13	75.2	2

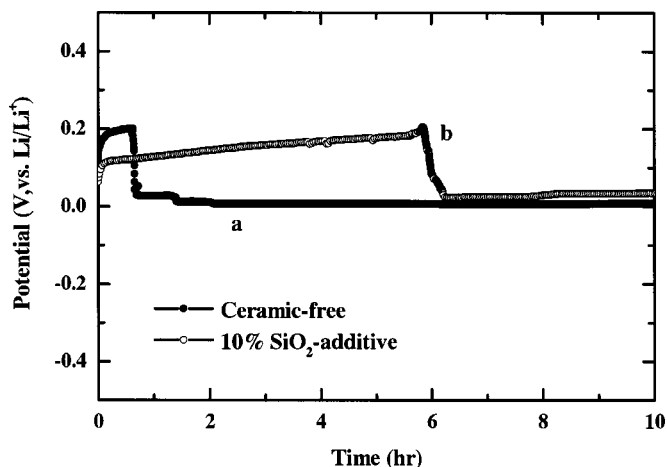


**Figure 4.** Voltage profile of symmetric Li/solid polymer electrolyte/Li cell containing (a)  $(\text{PEO})_8\text{LiClO}_4$  and (b)  $(\text{PEO})_8\text{LiClO}_4 + 10\% \text{SiO}_2$  during galvanostatic pulses at  $0.4 \text{ mA/cm}^2$  at 60°C.

electrode. On other hand, it has been demonstrated that PEO is subject to oxidative attack, which results in degradation of the polymer, and this degradation is accelerated by certain heavy metal ions, certain oxidizing agents, acid, and ultraviolet light.<sup>17</sup> To verify whether or not the polymer decomposition is due to the presence of moisture, we conducted the following experiments: a coin-type cell of  $\text{Li}/\text{Li}_x\text{MnO}_2$  containing the ceramic-free electrolyte was well sealed in an aluminum-laminated cell. This showed a major improvement in the cycle life compared with the simple coin-cell, as shown in Fig. 7A. It is reasonable to understand that the improvement is due to reduced water adsorption, thus decreasing the lithium passivation film growth and PEO decomposition. We further used a multiple film consisting of a high molecular weight branched  $\text{PEO}(\text{EO}/\text{EM}-2/\text{AGE})\text{-LiN}(\text{CF}_3\text{SO}_2)_2$  electrolyte film (next to the cathode side) together with the PEO-based electrolyte film instead of the single PEO electrolyte film, then assembled a  $\text{Li}/\text{Li}_x\text{MnO}_2$  coin cell. The extra charge capacity disappeared upon cycling, shows life enhancement, as curve (B) in Fig. 7. The excellent battery performance of a Li/polymer cell based on such a high molecular weight branched polymer electrolyte film has been described in detail in our previous studies.<sup>12,18</sup> We speculated that the interface between the Li/polymer interface would be same between using a

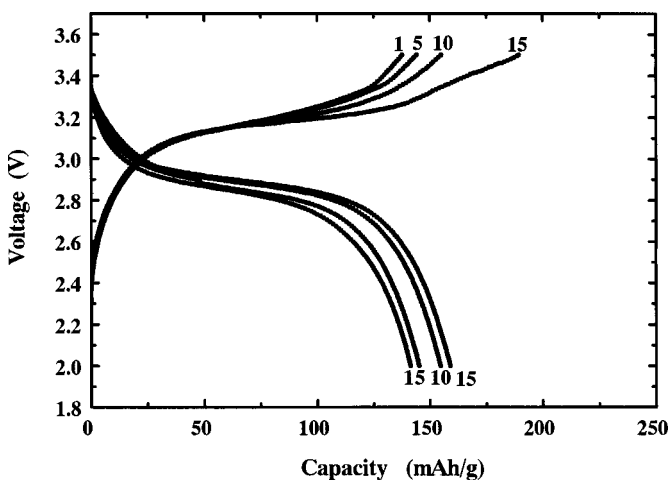


**Figure 5.** Charge/discharge curves of Li/solid polymer electrolyte/ $\text{Li}_{0.33}\text{MnO}_2$  containing ceramic-free polymer electrolyte for the first 15 cycles at 60°C. The charge/discharge current density is  $0.25 \text{ mA/cm}^2$ .

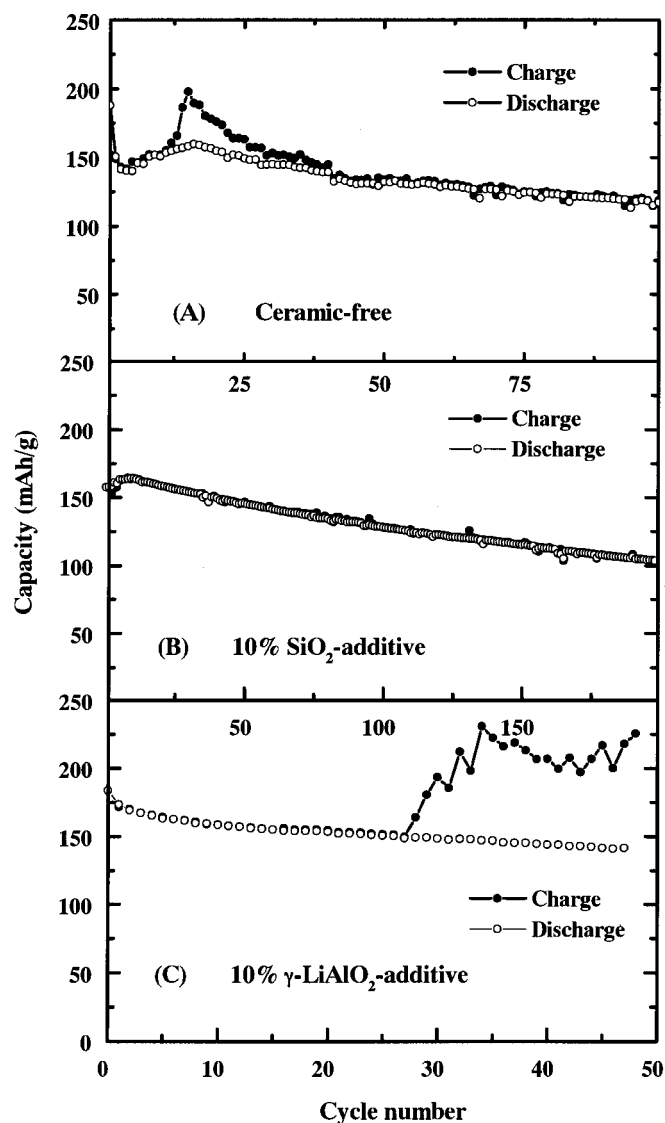


**Figure 6.** A plot of charge/discharge capacity vs. cycle number of Li/solid polymer electrolyte/ $\text{Li}_{0.33}\text{MnO}_2$  cell containing various electrolyte membranes at  $60^\circ\text{C}$ . (A)  $(\text{PEO})_8\text{LiClO}_4$ , (B)  $(\text{PEO})_8\text{LiClO}_4 + 10\% \text{SiO}_2$ , and (C)  $(\text{PEO})_8\text{LiClO}_4 + 10\% \gamma\text{-LiAlO}_2$ . The charge/discharge current density is  $0.25 \text{ mA/cm}^2$ .

single PEO polymer film and multiple films, the enhanced stability against oxidation was thereby most likely due to a stable PEO chain by the branch effect, thus suppressing the PEO decomposition, rather than decreasing the adsorbed water content. For a ceramic-free electrolyte, it is reasonable to understand that PEO slowly adsorbs water to react with the lithium salt, giving rise into an acid medium, thus facilitating the polymer degradation during charge. When the oxidation film reached a certain thickness, the decomposition will stop. These results suggested that the PEO decomposition can be suppressed either by a decrease in adsorbed water (preventing formation of an acid medium) or maintaining a stable PEO chain structure. We considered that the influence of adsorbed water being present in the PEO-based polymer electrolyte on its electrochemical stability is much more pronounced at the cathode rather than at the lithium electrode.

Scrosati *et al.* have confirmed that the increase in conductivity by ceramic modification was due to interactions induced via Lewis acid/base reactions between the ceramic surface and the PEO segments, and the Lewis acid groups of the added ceramics (*e.g.*,  $-\text{OH}$

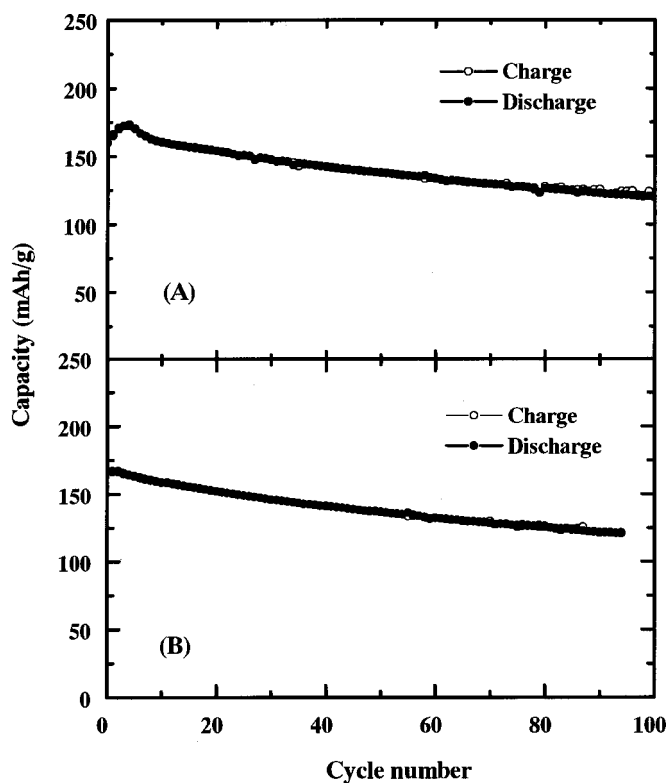


**Figure 7.** Cycle life of Li/solid polymer electrolyte/ $\text{Li}_{0.33}\text{MnO}_2$  cell at  $60^\circ\text{C}$ . (A) a coin-type cell sealed in an aluminum-laminated cell containing  $(\text{PEO})_8\text{LiClO}_4$  electrolyte, (B) coin-type cell containing  $(\text{PEO})_8\text{LiClO}_4$  and a high molecular weight branched polymer electrolyte. The charge/discharge current density is  $0.25 \text{ mA/cm}^2$ .

groups on the  $\text{SiO}_2$  surface) form complexes with the PEO chains.<sup>19</sup> We speculate that the Lewis acid/base interaction not only lowers the polymer chain reorganization tendency, but also stabilizes its structure. The strong Lewis acid/base reaction was also effective in the ferroelectric ceramic-modified composite electrolyte due to the permanent dipole, thus reducing or suppressing the PEO decomposition.<sup>4</sup> Unfortunately, we could not explain why some ceramics, *e.g.*, inorganic lithium salts, show improved lithium/polymer interfacial stability, but cannot suppress the PEO decomposition. Which the inorganic lithium salts may dissociate into lithium ion and anion, behaving in the same manner as the lithium salt electrolyte, it has no stabilization effect. The PEO decomposition mechanism is quite complicated, and we cannot claim that the reason responsible for the influence of the ceramic additive on its electrochemical profile has been clarified, therefore, much more work should be carried out. However, as an evaluation method, it is necessary and important to assemble a real lithium/polymer battery and monitor its cycle life.

Figure 8 shows the discharge curves of a  $\text{Li}/\text{Li}_x\text{MnO}_2$  containing an  $\text{SiO}_2$ -additive polymer electrolyte at temperatures varying from  $40$  to  $80^\circ\text{C}$ . The cell could be operated at  $40^\circ\text{C}$ , and delivered a capacity of  $75 \text{ mAh/g}$  at  $0.1 \text{ mA/cm}^2$ , corresponding to a 44% initial utilization of the  $\text{Li}_x\text{MnO}_2$ . Figure 9 illustrates the discharge capacity of a  $\text{Li}/\text{Li}_x\text{MnO}_2$  cell at various rates. The cell was discharged to  $2.0 \text{ V}$  at various discharge currents from  $0.03$  to  $0.75 \text{ mA/cm}^2$ . The charge current density was always set at  $0.1 \text{ mA/cm}^2$ . For the active material mass loading in the composite electrode (*ca.*  $5 \text{ mg/cm}^2$ ), the current selected here corresponded to a 1/40 to 1 h discharge rate. Under optimized conditions, the system exhibits a very good rate capability; it delivers a capacity of about  $160 \text{ mAh/g}$  of  $\text{Li}_x\text{MnO}_2$  at

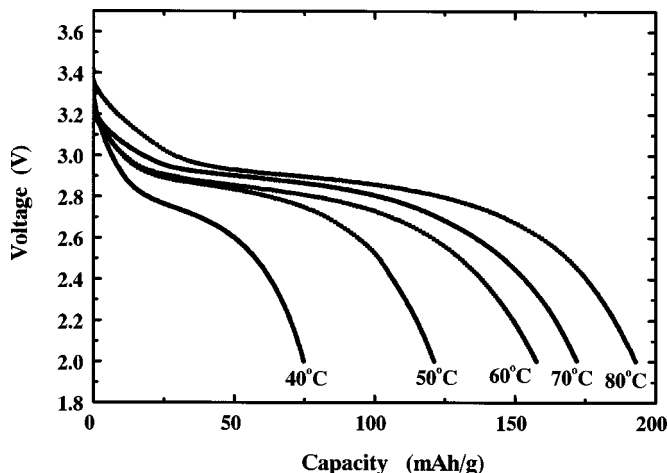


**Figure 8.** Discharge curves of Li/solid polymer electrolyte/ $\text{Li}_x\text{MnO}_2$  cell at various operating temperatures: 40°C, 50°C, 60°C, 70°C, and 80°C. The discharge current was 0.1 mA/cm<sup>2</sup>.

the C/3 rate, corresponding to a specific energy of 450 Wh/kg of the pure oxide.

### Conclusion

We have evaluated the electrochemical profile of an all solid-state  $\text{Li}/\text{Li}_x\text{MnO}_2$  polymer battery using various ceramic modified PEO- $\text{LiClO}_4$  composite electrolytes, namely metal oxides and inorganic lithium salts, as well as ferroelectrics ceramics. The addition of ceramics resulted in an enhancement of the ionic conductivity,

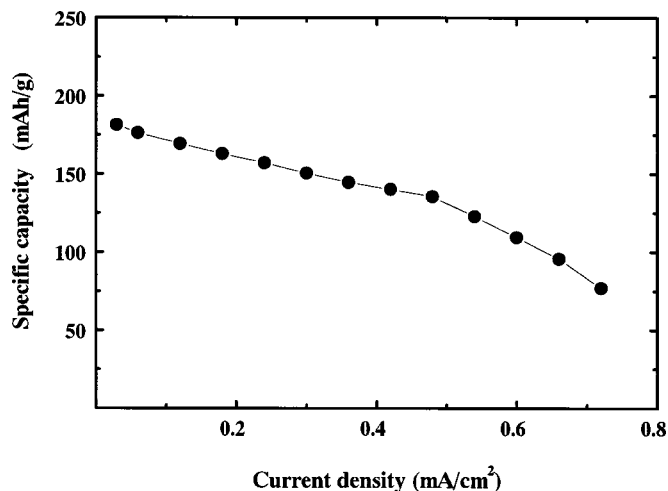


**Figure 9.** Discharge capacity of Li/solid polymer electrolyte/ $\text{Li}_x\text{MnO}_2$  cell at various current rates from 0.03 to 0.75 mA/cm<sup>2</sup> and 60°C. The charge current was always 0.1 mA/cm<sup>2</sup>. Cells were cycled between 2.0 and 3.5 V.

especially at temperatures below the crystalline-amorphous transition (normally at 60°C), and showed a higher interface stability with lithium metal and a stronger mechanical property.

An all solid-state  $\text{Li}/\text{Li}_x\text{MnO}_2$  based on a ceramic-free PEO- $\text{LiClO}_4$  electrolyte showed an extra charge capacity over discharge capacity during cycling, which is most likely due to the decomposition of PEO toward the cathode in presence of moisture. The PEO decomposition suppression was observed on these doped components that form a stable interaction between the ceramic surface and the PEO segment, e.g., the metal oxides, thus stabilizing the PEO structure, and protecting the PEO oxidation. However, some ceramic-modified composite polymer electrolytes (inorganic lithium salts) behave in the manner similar to that of the ceramic-free polymer electrolyte, even if they also show improved lithium/polymer interface stability. Accordingly, we suggested that it is necessary and important to assemble a real lithium/polymer battery to evaluate the polymer electrolytes.

An all solid-state  $\text{Li}/\text{Li}_x\text{MnO}_2$  containing the  $\text{SiO}_2$ -additive polymer electrolyte delivers a rechargeable capacity of 160 mAh/g of  $\text{Li}_x\text{MnO}_2$  with a very flat working voltage plateau at ca. 3.0 V vs.  $\text{Li}/\text{Li}^+$  at the C/3 rate at 60°C corresponding to a specific energy of 450 W/kg of active material, and also showed good rate capability and excellent cyclability.

### Acknowledgments

The authors would like to thank the Japan Science and Technology Corporation (JST) for partially funding the project. The authors also thank Daiso Co., Ltd., for furnishing the polymer-electrolyte, Nippon Sheet Glass Co., Ltd., NFG Company for the ceramic additives, and Chuo Denki Kogyo Co., Ltd., for  $\text{Li}_{0.33}\text{MnO}_2$ . The authors also gratefully acknowledge Dr. T. Takeuchi of the Green Life Technology Research Team of the same institute for the useful discussion.

The National Institute of Advanced Industrial Science and Technology Kansai Collaboration Center assisted in meeting the publication costs of this article.

### References

1. M. B. Armand, J. M. Chabagno, and M. J. Duclot, in *Fast Ion Transport in Solids*, P. Vashita, J. N. Mundy, and G. K. Shenoy, Editors, p. 131, North-Holland, Amsterdam (1979).
2. J. Przulski, K. Such, H. Wycislk, and W. Wieczorek, *Synth. Met.*, **35**, 241 (1990).
3. F. Croce, G. B. Appetechi, L. Persi, and B. Scrosati, *Nature (London)*, **394**, 456 (1998).
4. H. Y. Sun, H. J. Sohn, O. Yamamoto, Y. Takeda, and N. Imanishi, *J. Electrochem. Soc.*, **146**, 1672 (1999).
5. M. Watanabe and A. Nishimoto, *Solid State Ionics*, **79**, 306 (1995).
6. S. Sylla, J. Y. Sanchez, and M. Armand, *Electrochim. Acta*, **37**, 1699 (1992).
7. G. Negasuramanian, E. Peled, A. I. Attia, and G. Halpert, *Solid State Ionics*, **67**, 51 (1993).
8. Y. Dai, Y. Wang, S. G. Greenbaum, S. A. Bajue, D. Golodnitsky, G. Ardel, E. Strauss, and E. Peled, *Electrochim. Acta*, **10-11**, 1557 (1998).
9. E. Peled, D. Golodnitsky, G. Ardel, J. Lang, and Y. Lavi, *J. Power Sources*, **54**, 496 (1995).
10. D. E. Strauss, D. Golodnitsky, and E. Peled, *Electrochem. Solid-State Lett.*, **2**, 115 (1999).
11. M. Yoshio, H. Nakamura, and Y. Xia, *Electrochim. Acta*, **45**, 273 (1999).
12. Y. Xia, T. Fujieda, K. Tatsumi, P. P. Prosini, and T. Sakai, *J. Electrochem. Soc.*, **147**, 2050 (2000).
13. E. Quartarone, P. Mustarelli, and A. Magistris, *Solid State Ionics*, **110**, 1 (1998).
14. F. B. Dias, L. Plomp, and J. B. J. Veldhuis, *J. Power Sources*, **88**, 169 (2000).
15. J. E. Weston and B. H. C. Steel, *Solid State Ionics*, **7**, 75 (1982).
16. B. Kumar and L. G. Scanlon, *Solid State Ionics*, **124**, 239 (1999).
17. F. E. Bailey, Jr. and J. V. Koleske, *Poly(ethylene oxide)*, p. 53, Academic Press, Inc., (1976).
18. Y. Xia, T. Sakai, C. Wang, T. Fujieda, K. Tatsumi, K. Takahashi, A. Mori, and M. Yoshio, *J. Electrochem. Soc.*, **148**, A112 (2001).
19. B. Scrosati, F. Croce, and L. Persi, *J. Electrochem. Soc.*, **147**, 1781 (2000).